ELSEVIER

Biochimica et Biophysica Acta 1366 (1998) 301–316

BIOCHIMICA ET BIOPHYSICA ACTA
BBA

The LH1–RC core complex of *Rhodobacter sphaeroides*: interaction between components, time-dependent assembly, and topology of the PufX protein

Rachel J. Pugh, Peter McGlynn, Michael R. Jones, C. Neil Hunter *

Robert Hill Institute for Photosynthesis and Krebs Institute for Biomolecular Research, Department of Molecular Biology and Biotechnology, University of Sheffield, Western Bank, Sheffield S10 2TN, UK

Received 12 March 1998; revised 19 May 1998; accepted 27 May 1998

Abstract

Mutant strains of the photosynthetic bacterium *Rhodobacter sphaeroides*, lacking either LH1, the RC or PufX, were analysed by mild detergent fractionation of the cores. This reveals a hierarchy of binding of PufX in the order RC:LH1 > LH1 > RC. The assembly of photosynthetic membranes was studied by switching highly aerated cells to conditions of low aeration in the dark. The RC-H subunit appears before other components, followed by the *pufBALMX* then *pufBA* transcripts. Synthesis of the PufX polypeptide precedes that of LH1α and β, which suggests that PufX associates with a limited amount of LH1α, β and the RC, and prior to the encirclement of the RC by the rest of the LH1 complex. The topology of PufX within the intracytoplasmic membrane was determined by proteolytic treatment of membrane vesicles followed by protein sequencing; PufX is N-terminally exposed on the cytoplasmic surface of the photosynthetic membrane.

Keywords: Membrane protein; Assembly; Light harvesting; Reaction center; Photosynthesis; PufX

1. Introduction

The photosynthetic bacterium *Rhodobacter (Rb.) sphaeroides* is an excellent model organism for the study of the assembly and organisation of the photosynthetic apparatus, having a relatively simple photosystem consisting of a single type of reaction centre (RC), plus two types of light-harvesting complex. The peripheral light harvesting complex (LH2) is present in variable amounts in the cell depending on the incident light intensity, whereas the core light harvesting complex (LH1) is present in a fixed stoichiometry to the RC [1]. The organisation of the photosystem components enables captured light energy to be funnelled from the relatively high energy pigments of the LH2 antenna to the lower energy pigments of the LH1 antenna and of the RC. The LH complexes thereby increase the efficiency of light absorption by the RC, the site of primary photochemistry. Upon transfer of the captured excitation

Abbreviations: *Rb.*, *Rhodobacter*; *Rps.*, *Rhodopseudomonas*; RC, reaction centre; LH1, light harvesting antenna system 1; LH2, light harvesting antenna system 2; Bchl, bacteriochlorophyll; MLH1/RC, LH1:RC ratio in intracytoplasmic membranes; SLH1/RC, LH1:RC ratio in detergent solubilised complexes; λ_{max} absorbance maximum; prot K, proteinase K; cyt, cytochrome; PMSF, phenylmethylsulphonyl fluoride

* Corresponding author. Fax: +44 (114) 272-8697; E-mail: c.n.hunter@sheffield.ac.uk

0005-2728/98/$ – see front matter
PII: S0005-2728(98)00131-5

energy to the RC, cyclic electron transfer occurs via a membrane-bound pool of ubiquinone, the cytochrome (cyt) bc_1 complex and a soluble cyt c_2 in the periplasmic space. The net result of these energy and electron transfer processes is the transfer of protons from the cytoplasmic side of the membrane to the periplasmic side, generating a proton electrochemical gradient.

The structures of the RCs of *Rhodopseudomonas viridis* and *Rb. sphaeroides* have been determined at atomic resolution by X-ray crystallography [2–5]. More recently, similar progress has been made for the LH2 complexes of *Rhodopseudomonas acidophila* strain 10050 [6] and *Rhodospirillum molischianum* [7]. Cryo-electron microscopy has also made important contributions to our understanding of the structure of LH complexes [8–14]. Circular structures were seen for both the LH1 and LH2 complexes at resolutions of 26–8 Å. LH2 is composed of two small hydrophobic peptides designated α and β. These each have a single membrane-spanning helix and together form ligands to one 800 nm bacteriochlorophyll *a* (Bchl) and two 850 nm Bchl molecules to form an αβ heterodimer. The information at atomic resolution [6] shows that the *Rhodopseudomonas acidophila* LH2 complex consists of nine circularly arranged αβ heterodimers forming a hollow cylinder that spans the membrane. The Bchl molecules also form two rings, a nine-member ring of 800 nm Bchls (B800), and an 18-member ring of 850 nm Bchls (B850). The crystal structure of LH2 from *Rhodospirillum molischianum* [7] consists of a similar cylindrical arrangement of eight αβ heterodimers, with an eight-member ring of B800 Bchls and a 16-member ring of B850 Bchls. This circular arrangement of B850 Bchls is thought to allow any excitation arising from incident light to become rapidly delocalised over a number of adjacent Bchls and to facilitate efficient energy transfer to an adjacent LH1 (or LH2) complex. Evidence based on low resolution electron microscopy data for the core light harvesting complex, LH1, of *Rhodospirillum rubrum*, suggests that the LH1 complex is also organised into cylinders of 16 αβ heterodimers in a similar manner to the LH2 complex [8], and it is proposed that the Bchls of LH1 (which absorb at 880 nm) are arranged in an overlapping 32-member ring in a manner that is analogous to the 850 nm Bchls of LH2. The precise spatial relationship of the LH2, LH1 and RC complexes within the bacterial photosystem remains unknown; however, it has been noted that there is probably sufficient space for a single RC complex to reside within the ring of the *Rhodospirillum rubrum* LH1 complex [8]. Evidence for the presence of the RC within a ring of LH1 is also supported by low resolution electron microscopy images of the *Rhodospirillum molischianum* RC–LH1 core complex, although it was proposed that there were only 12 αβ heterodimers within the LH1 ring in this species [13], and two-dimensional LH1–RC crystals from *Rhodospirillum rubrum* [14] whose geometry and subunit stoichiometry strongly suggest that the gross conformation of the LH1 ring is unaffected by the presence of the RC.

The structural genes encoding the *Rb. sphaeroides* LH1α and β polypeptides (*pufA* and *pufB*), and the RC L and M subunits (*pufL* and *pufM*) reside within the *puf* operon, which contains six genes transcribed in the order *pufQBALMX* [15–18]. *PufQ* has an important, but unknown, role in Bchl biosynthesis [18,19] and *pufX* has been shown to encode a protein essential for maintaining the capacity of the RC–LH1 core complex to support photosynthetic growth. It is possible that this is achieved by facilitating a sufficiently high rate of exchange of ubiquinone/ubiquinol between the RC and the cyt bc_1 complex in the presence of the LH1 antenna [20–24]. Expression of the *puf* operon in *Rb. sphaeroides*, and the closely related bacterium *Rb. capsulatus*, is very complex and involves regulation of both transcription and mRNA degradation. Two major *puf* operon transcripts of 0.5 and 2.7 kb can be detected [25]; the 0.5 kb mRNA encodes *pufBA* and is present in a 10–15-fold molar excess over the 2.7 kb transcript, which encodes *pufBALMX* [26]. This excess of *pufBA*-specific transcripts over *pufLM* mRNA is a major determinant of the LH1:RC stoichiometry in the photosystem. A putative stem-loop structure in the mRNA between *pufA* and *pufL* is suggested to control the relative levels of the 0.5 and 2.7 kb *puf* operon transcripts [27,28]. In *Rb. sphaeroides*, there is evidence that this stem-loop acts as an efficient transcription terminator which allows only limited transcription of *pufLMX* [27,29]. However, the *pufA–L* stem-loop in *Rb. capsulatus* has been shown to impede 3′–5′ exoribonuclease attack on the *pufBA* region of *pufBALMX* transcripts and so the molar ex-

cess of *pufBA* mRNA is due to enhanced stability of this region of *pufBALMX* mRNA [30,31].

The additional open reading frame downstream of *pufM*, which is transcribed as part of the polycistronic *puf* mRNA and termed *pufX* in both *Rb. capsulatus* [32] and *Rb. sphaeroides* [26,29], has been shown to be essential for photosynthetic growth [20,21]. However, the precise role of the 9 kDa PufX protein, which is shown to be located in the intracytoplasmic membrane and associated with the RC–LH1 core complex in *Rb. sphaeroides* [20], remains unknown. The observation that PufX is vital for photosynthetic growth only in strains that contain the LH1 antenna [22] is compatible with proposals that this protein may function to organise the macromolecular structure of the photosynthetic membrane such that ubiquinol/ubiquinone exchange can occur between the RC and cyt bc_1 complexes [20–24]. Furthermore, it would appear that the ratio of LH1 to RC in the core complex in some way determines whether the presence of PufX is essential for photosynthetic growth in mutant strains [33].

A number of mutations that suppress the photosynthetic-minus phenotype of strains lacking *pufX* [21,34,35] have been mapped to the *pufBA* genes that encode the LH1 polypeptides. Many of these suppression mutations lead to reduced levels of LH1 relative to the RC [35]. This again demonstrates that a reduction in size of the antenna through macromolecular reorganisation restores the capacity of the bacterium for photosynthetic growth. However, it is noted that not all such suppression mutations mapped to the *pufBA* region, and those that did were expressed in the presence of unmutated chromosomal versions of *pufB* and *pufA*, as the strains were constructed in the presence of both chromosomal and plasmid borne LH1 genes. In an independent study, two suppressor mutants of *Rb. capsulatus* [36] which were more accurately designated partial suppressor mutations due to the less efficient use of light energy when compared to the pseudo-wild-type, were also shown to possess a less stable photosynthetic apparatus. The mutations were mapped to Ser^{30} of LH1α, and these data suggest that this Ser residue determines functionally important interactions of the LH1α polypeptide. Taken together, these studies support the idea that PufX plays a central role in the organisation of the RC–LH1 core complex.

One aim of the present study was to examine the association of PufX with the other components of the core, the LH1 and RC complexes, both in wild-type cores and cores containing reduced levels of LH1 with respect to RC. It is possible to bring about changes in the stoichiometry of LH1:RC without the secondary effect of changes in the amino acid sequence of LH1α or β that could also alter the conformation of the complex [33]. It has been shown previously that deletion of the stem-loop structure immediately downstream of *pufA* caused an apparent decrease in the LH1:RC ratio in both *Rb. sphaeroides* and *Rb. capsulatus* [27,30]. Accordingly, in the present study the major stem-loop downstream of *pufA* has been deleted and the phenotype of the resulting mutant strain has been determined. We find that the stem-loop deletion mutant has RC–LH1 core complexes which have a reduced number of LH1 Bchls per RC, in addition to a significant level of free RCs.

Previously, Niederman et al. [37] showed that the assembly of photosynthetic membranes can be studied in vivo by inducing the synthesis of the components of the photosystem in the dark under oxygen-limiting conditions. Another aim of the present study was to use a similar approach in order to gain an insight into the relationship of the components of the RC:LH1 core complex, and the sequence of assembly of PufX in relation to the rest of the core. Moreover, a direct, time-based comparison of mRNA transcripts and protein extracts was performed to study the relationship of both transcript levels and encoded protein in vivo. The results obtained in the present work confirm that the RC-H subunit protein is constitutively present in the membrane at low levels even before photosynthetic growth is induced, as first proposed by Chory et al. [38], and demonstrate that PufX and the LH proteins are present in the membrane after a initial lag, with the presence of PufX being more immediate and rising more rapidly after the induction of photosynthetic membrane synthesis. This suggests that the PufX protein is a vital and early component in the assembly process.

Finally, this study aimed to determine the topology of PufX within the membrane using proteinase K (prot K) treatment of chromatophore membranes and N-terminal microsequencing. Analysis of the

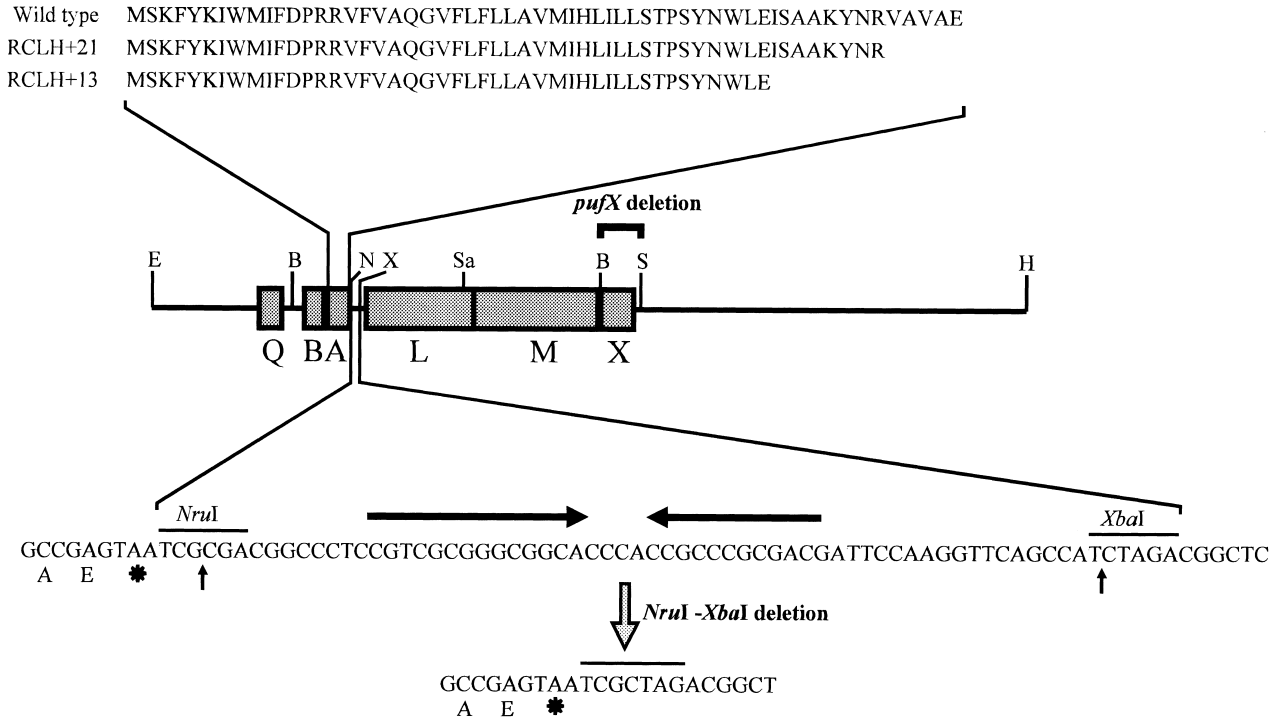

Fig. 1. Top: arrangement of the wild-type *puf* operon and the nature of the truncation mutants RCLH+21 and RCLH+13. Bottom: construction of a mutant *puf* operon lacking the putative stem-loop structure between *pufA* and *pufL*. Engineered *Nru*I and *Xba*I sites downstream of *pufA* [41] flank the stem-loop region, indicated by horizontal arrows [27]. Restriction at these sites, filling in of the recessed 3′ ends and subsequent ligation of the blunted sites allowed deletion of the stem-loop structure. The sequence of the resulting junction is shown (horizontal bar), together with the final two codons and the stop codon of *pufA*. The deletion of the *Bam*HI–*Sma*I fragment encompassing *pufX*, in RCLH12X$^-$ and ΔTΔX, is also shown. Restriction sites are: E, *Eco*RI; B, *Bam*HI; N, *Nru*I; X, *Xba*I; Sa, *Sal*I; S, *Sma*I; H, *Hin*dIII.

PufX peptide has shown that it consists of 83% hydrophobic and neutral residues, suggesting it to be an intrinsic membrane protein. Hydropathy plots indicate that PufX possesses a putative membrane-spanning region of 25 amino acids [29]. Our results suggest that the N-terminus of PufX is exposed on the cytoplasmic surface of the membrane. Such an orientation, N_{in}–C_{out}, would be consistent with the prediction made using von Heijne's 'positive-inside' rule [39], based upon the number of positive charges in the N- and C-terminal regions.

2. Materials and methods

2.1. Bacterial strains, plasmids, gene transfer and growth conditions

All bacterial strains, plasmids and growth conditions were as described previously [33] except wild-type *Rb. sphaeroides* NCIB 8253 (R.A. Niederman), and mutants ΔT and ΔTΔX which are described below. Conjugative transfer of plasmids from *Escherichia coli* to *Rb. sphaeroides* was performed as described in Hunter and Turner [40].

2.2. DNA manipulation

A DNA fragment encoding the putative stem-loop structure immediately downstream of *pufA*, and encompassed by engineered *Nru*I and *Xba*I sites, was deleted from plasmid pRKEK1H [41] (Fig. 1), which contains the *pufQ, B* and *A* genes and the 5′ end of the *pufL* gene. The *Eco*RI–*Sal*I fragment from the pRKEK1H derivative containing this deletion was then subcloned into plasmid pRKEH10 [42], which encodes the *pufQ*, *B*, *A*, *L*, *M* and *X* genes, to produce plasmid pΔT. This *Eco*RI–*Sal*I fragment containing the stem-loop deletion was also subcloned into plasmid pRKEH10X$^-$ [22], which encodes

pufQBALM, but has a deletion of the *pufX* gene, to form plasmid pΔTΔX.

Plasmids pRKEH10, pRKEH10X$^-$, pΔT and pΔTΔX were conjugated into *Rb. sphaeroides* strain DD13 to form strains RCLH12, RCLH12X$^-$, ΔT and ΔTΔX. In strain DD13, the *puc* operon (encoding the LH2 polypeptides) and the *puf* operon have been replaced by antibiotic resistance cassettes so that no chromosomally encoded LH2, LH1 or RC complexes are expressed [43]. This provided a null genetic background in which expression of the RC and LH1 complexes was dependent upon the plasmid-based copies of the *puf* operon.

2.3. Transcript analysis of mutants lacking the pufA–L stem-loop structure

To ascertain whether strains ΔT and ΔTΔX contained alterations in the pattern of *puf* transcripts that were similar to those seen by DeHoff et al. [27], a Northern blot of RNA isolated from cells grown semi-aerobically in the dark for 4 h was probed with a DNA fragment encoding *pufBA* (data not shown). This confirmed the pattern of transcription of strain ΔT to be similar to that found by DeHoff et al. [27] where deletion of the *pufA–L* stem-loop was shown to cause a decrease in the level of the large (2.7 kb) *pufBALMX* transcript, complete loss of the small (0.5 kb) *pufBA* transcript and an increased level of the minor 0.7 kb *pufBA* mRNA. In strain ΔTΔX, the pattern of transcription was similar to that of strain ΔT with the exception that the large transcript migrated at approximately 2.4 kb rather than 2.7 kb, as does the large transcript of strain RCLH12X$^-$. This decrease in transcript size reflects the deletion of 320 bp of DNA encompassing the *pufX* gene from the plasmid-based copies of the *puf* operon in these strains. As expected, this altered pattern of transcription led to a decrease in the LH1:RC ratio in these strains (see Fig. 3).

2.4. Induction of synthesis of the photosynthetic apparatus

Wild-type *Rb. sphaeroides* strain NCIB 8253 were grown overnight in the dark at 34°C in 2 l conical flasks containing 200 ml of M22+ medium (using 1 ml of a starter culture as an inoculum) with shaking at 250 rpm, which provides aeration sufficient to suppress synthesis of the photosynthetic apparatus. When the cells reached an A_{680} of 0.5–1.0 (approximately 14 h) they were harvested by centrifugation at 7000 rpm for 10 min at 4°C in a Beckman J-lite rotor and the cell pellet was resuspended in 5 ml of sterile M22+ medium. This cell suspension was used to inoculate a 100 ml conical flask containing 70 ml of M22+ medium to a final A_{680} of 2. These oxygen-limited cells were grown in the dark at 34°C with shaking at 160 rpm. Samples were taken in duplicate 0, 30, 60, 120, 240 and 360 min after inoculation into the 70 ml of medium for the preparation of RNA and protein (see below), and harvested by pelleting at 3000 rpm for 10 min in sterile Falcon tubes. Cell extracts for protein analysis of each time point were prepared by resuspension of the cell pellets in 200 μl of 10 mM Tris (pH 7.5) and the protein content determined. A sample from each time point equivalent to 240 μg of protein was then solubilised in the presence of SDS to a final concentration of 6.4% and was incubated at 65°C for 30 min. The samples were pelleted in a microfuge for 15 min at $12\,000 \times g$. The supernatant was carefully removed and mixed with SDS-PAGE solubilisation buffer.

2.5. RNA preparation

RNA was isolated from 40 absorbance units of cells (for example, 20 ml of $A_{680} = 2$) using the Ultraspec RNA isolation system (Biotecx, Texas, USA). RNA was separated on formaldehyde gels as described in Sambrook et al. [44] and transferred to Zeta Probe GT nylon membrane (Bio-Rad) by capillary transfer according to the manufacturer's recommendations. DNA probes were prepared using the Amersham Megaprime Kit and hybridisation was performed according to the recommendations of the Zeta Probe GT manufacturer.

2.6. Densitometry

Optical density measurements were performed on a Vilbur Lourmat densitometer. Several exposures of Northern and immunodetection autoradiograms were scanned in duplicate. The value recorded corresponded to the integrated intensity over the whole band, calculated as the 'volume' under each peak.

Optical density results from overexposed autoradiograms producing saturating peaks were discarded, and averages were calculated from all viable results. Errors were calculated as the standard error of the mean, and in all cases were less than 10% of the value of that mean.

2.7. Spectroscopy of intracytoplasmic membranes

All intracytoplasmic membranes were prepared as described in Jones et al. [45] with the exception of membranes prepared from photosynthetically grown wild-type cells for determination of PufX topology, which were prepared on continuous (5–35% w/w) sucrose gradients as described in Hunter et al. [46].

Absorbance spectroscopy of membrane samples was performed on a Guided Wave Model 260 spectrophotometer (Guided Wave, El Dorado Hills, CA, USA) and low temperature absorbance spectra were obtained on the same machine using a DN1704 liquid nitrogen cryostat (Oxford Instruments Limited, Oxford, UK). Absorbance measurements of acetone/methanol extracts of membranes were obtained on a Beckman DU 640 spectrophotometer (Beckman Instruments, High Wycombe, UK).

2.8. Sucrose gradients

Pigment–protein complexes from intracytoplasmic membranes were solubilised in 15 mM *n*-octyl-β-D-glucopyranoside and 15 mM deoxycholate and then separated by centrifugation on 10–40% sucrose gradients for 21 h as described by Molenaar et al. [47] and McGlynn et al. [33].

2.9. Calculation of RC concentration and the size of the LH1–RC core (LH1 Bchls per RC)

Ratios of LH1:RC in membrane samples and fractions from sucrose gradients of solubilised complexes were calculated as described in McGlynn et al. [22]. Extinction coefficients for the LH1 Q_y absorbance band of 123, 124, 102 and 109 mM^{-1} cm^{-1} were used for strains RCLH12 [33], RCLH12X$^-$ [33], ΔT and ΔTΔX respectively. These values used for strains ΔT and ΔTΔX were estimated using the method as described in McGlynn et al. [33]. The percentage of free RCs in fractions from sucrose gradients was calculated as described in McGlynn et al. [33].

2.10. Measurement of Bchl and RC concentration per cell

Two independent cultures of each *Rb. sphaeroides* strain were grown to early stationary phase in 70 ml of medium in 100 ml conical flasks at 34°C and 160 rpm in the dark. Pigments were then extracted from 20 and 50 μl samples of each culture by mixing with 1 ml of acetone/methanol (7:2, v/v) in the dark, cell debris was removed by centrifugation for 5 min and the Bchl concentration calculated using the method of van der Rest and Gingras [48]. The absorbance at 680 nm of the cell culture immediately prior to extraction was used to estimate the number of cells extracted, based on an absorbance of 1 being equivalent to 1×10^9 cells ml^{-1}, and used together with the calculated Bchl concentration to estimate the amount of Bchl per cell. The RC concentration per cell was calculated from the Bchl concentration per cell and the estimated LH1:RC ratio for intracytoplasmic membranes of the relevant strain.

2.11. Sodium dodecyl sulphate polyacrylamide gel electrophoresis and immunoblotting

Protein samples were separated on a 16.5% polyacrylamide gel according to the method of Schägger and von Jagow [49], and stained with Coomassie blue. Total protein was determined using the bicinchoninic acid (Sigma) method [50]. Transfer of proteins to Hybond C (Amersham) and incubation of the blot were performed according to standard methods [44]. Proteins were detected using horseradish peroxidase conjugated goat anti-rabbit antisera and enhanced chemiluminescence detection reagents supplied by Amersham. The antibodies were kindly supplied by the following: LH1, LH2 (Prof. R.J. Cogdell, Glasgow University, UK), subunit IV of the cyt bc_1 complex and subunit H of the RC (Prof. R.A. Niederman, Rutgers University, USA).

2.12. Proteinase K treatment of chromatophore membranes from the wild-type strain

Chromatophores were treated with prot K at an

enzyme to membrane protein ratio of 1:30 in 10 mM Tris (pH 7.5) for increasing lengths of time at 30°C. After the desired time interval (0, 5, 10, 20, 40, 60, 80 and 100 min) the proteolysis reaction was terminated by the addition of phenylmethylsulphonyl fluoride (PMSF) to a final concentration of 0.5 mM at 0°C. The samples were then flash frozen on dry ice, solubilisation buffer was added, and the samples were incubated at 65°C for 15 min prior to SDS-PAGE.

2.13. N-terminal microsequencing for amino acid sequence determination

Protein samples used for N-terminal sequence determination were separated by SDS-PAGE as described and then electroblotted on to PVDF membranes (ProBlott, Applied Biosystems) using CAPS buffer according to the method of LeGendre and Matsudaira [51]. The gel was blotted onto PVDF sequencing membrane, stained with Coomassie blue R-250 and destained with 50% methanol. In order to locate PufX and enable the correct bands to be excised from the sequencing membrane for analysis a duplicate gel was blotted onto Hybond C nitrocellulose (Amersham) for Western analysis and the immunoreactive bands were highlighted by alkaline phosphatase colour immunodetection. Bands were excised and the N-terminal sequence determined by sequential Edman degradation using an ABI 476A sequencer. Phenylthiohydantoin derivatives were analysed with an on-line detector calibrated with 12 pmol of each PTH amino acid [51].

3. Results

3.1. Biochemical characterisation of the pufA–L stem-loop deletion strains

Deletion of the *pufA–L* intercistronic loop in the strains ΔT and ΔTΔX led, as expected [27], to the loss of the 0.5 kb transcript and the appearance of a 0.7 kb transcript. On the basis of the data in DeHoff et al. [27], the perturbation of *puf* operon transcripts in these strains was expected to lead to a decrease in the LH1:RC ratio. In order to examine this directly, absorbance spectra of intracytoplasmic membranes were recorded at 77 K, normalised with respect to the 800 nm absorbance band arising from the RC, and compared with spectra of the control strains RCLH12 and RCLH12X$^-$ (Fig. 2). The increase in the relative intensity of the LH1 Q_y absorbance band in membranes of strain RCLH12X$^-$ (as compared with those from strain RCLH12), has been reported previously and has been attributed to a small increase in the LH1:RC ratio due to the lack of PufX in the RCLH12X$^-$ strain [22]. Comparison of spectra of strains ΔT and ΔTΔX with those of the control strains showed that, as expected, strains lacking the *pufA–L* stem-loop had a reduced level of LH1 with respect to the RC. The ratio of LH1:RC was estimated from these spectra as described in Section 2, and is shown in Table 1 (denoted as MLH1/RC). The number of LH1 Bchls per RC fell to approximately 14 and 12 for ΔT and ΔTΔX, respectively.

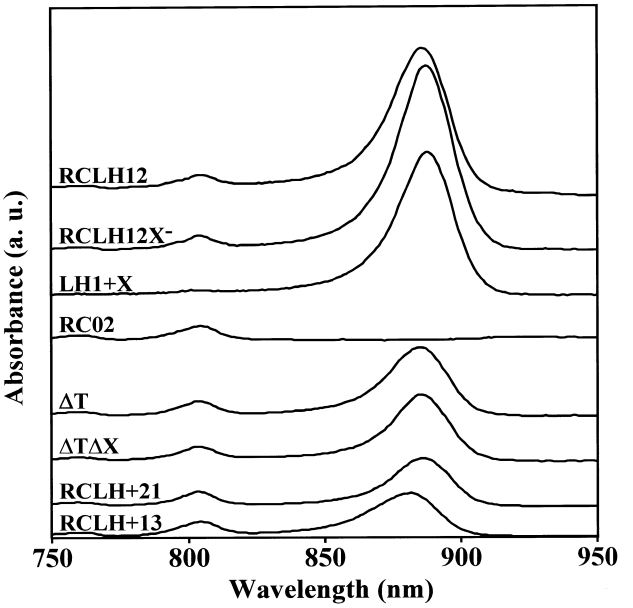

Fig. 2. Absorbance spectra of the control and mutant strains at 77 K. The spectra were normalised to an absorbance of 0.1 for the 800 nm RC peak in all strains, except for the LH1+X strain which was normalised to an equal amount of Bchl to that in the RCLH12 control strain.

In addition to the effects on the ratio of LH1:RC, the absolute levels of both LH1 and the RC were also altered in strains ΔT and ΔTΔX. The level of total Bchl per cell for strains ΔT and ΔTΔX was reduced to about 40% of that found in the control strains, and the number of RCs per cell in strains ΔT and ΔTΔX was reduced to 60 and 70%, respectively,

of that seen in the control strains (Table 1). The simplest explanation for this effect is that deletion of the *pufA–L* stem-loop causes a decrease in expression of *pufLM*, and hence a decrease in the level of RC synthesis.

3.2. Demonstration of a heterogeneous population of RCs in the 'small core' mutant ΔT and dissociation of PufX from the LH1–RC complex

The availability of the ΔT strain provides an opportunity to look for heterogeneity in the organisation of the RC–LH1 core system. There is a precedent for such heterogeneity; in a previous publication [33], mild detergent treatment of membranes followed by centrifugation of the solubilised material on a continuous sucrose gradient was used to show that strains that had a decreased ratio of LH1:RC (RCLH+21 and RCLH+13) also had a significant population of antenna-free RCs. The same approach was used to examine the composition of membranes from the strains used in the present study. The amount of RCs and LH1 present in aliquots taken from sucrose gradients was determined by immunoblotting of proteins separated by SDS-PAGE as described in Section 2.

The mutants studied fell into two categories: those in which either the LH1, X or RC component of the core was absent, or those in which the stoichiometry of LH1 and RC had been altered, either by removal of the intercistronic stem-loop structure (see Section 3.1) or by progressive truncation of the C-terminus of the LH1α polypeptide [33]. The C-terminal deletion strains RCLH+21 and RCLH+13 studied here were selected from a larger group of C-terminal truncation mutants [33]. RCLH+21 and RCLH+13 represent a contrast in core size and ability to maintain photosynthetic growth in the absence of PufX, and are truncated at the C-terminus of the LH1α polypeptide by 5 and 13 residues, respectively.

Each of the strains ΔT, RCLH+21 and RCLH+13 possesses a similar characteristic, in that they have a reduced ratio of LH1:RC, as calculated from spectra of intracytoplasmic membranes (Fig. 2 and Table 1). These data further suggest that the stability of the PufX protein is due to post-translational factors, and that the increase in the level of PufX is connected in some way to the decrease in the ratio of LH1:RC in the membrane. This increase in the level of the PufX protein on reduction of the amount of LH1 per RC was seen irrespective of the method used to bring about this reduction in the relative level of LH1, being observed in strain ΔT where LH1α and β are wild-type polypeptides, and in strains RCLH+21 and RCLH+13 where LH1α is truncated at the C-terminus.

Fig. 3 shows the result of this analysis, which included the LH1 and RC deficient strains, RCO2 and LH1+X respectively; these strains are controls for the migration of individual RC and LH1 complexes in the sucrose gradient. In the absence of LH1, the main fraction of RCs in the RCO2 mutant strain was restricted to between 10 and 20% sucrose, and termed 'free RCs', in contrast to the LH1 and RC–LH1 complexes in the LH1+X and RCLH12 strains, respectively, which migrated to higher sucrose concentrations. It was estimated that approximately 25% of the RCs in strain ΔT were unconnected to LH1, compared with less than 5% for the control strain RCLH12 (Table 1). These results show that although

Table 1
Summary of spectroscopic and biochemical data for control and stem-loop deletion strains

Strain	Cells		Membranes		Solubilised complexes		
	Bchl/cell[a] ($\times 10^{18}$ mol)	RC/cell[a] ($\times 10^{19}$ mol)	MLH1/RC	LH1 λ_{max} [b] (nm)	SLH1/RC	LH1 λ_{max} [b] (nm)	% Free RC[c]
RCLH12	2.9 ± 0.1	1.0	25.7 ± 3.2	888	29 ± 1	886	2
RCLH12X$^-$	3.3 ± 0.5	1.0	27.8 ± 3.2	888	29 ± 2	886	6
ΔT	1.1 ± 0.1	0.6	14.5 ± 1.5	888	21 ± 3	886	22
ΔXΔT	1.2 ± 0.3	0.7	12.2 ± 0.6	887	19 ± 2	885	20

[a]Calculated for cells grown semi-aerobically in the dark.
[b]Calculated from 77 K spectra.
[c]Relative to LH1+X.

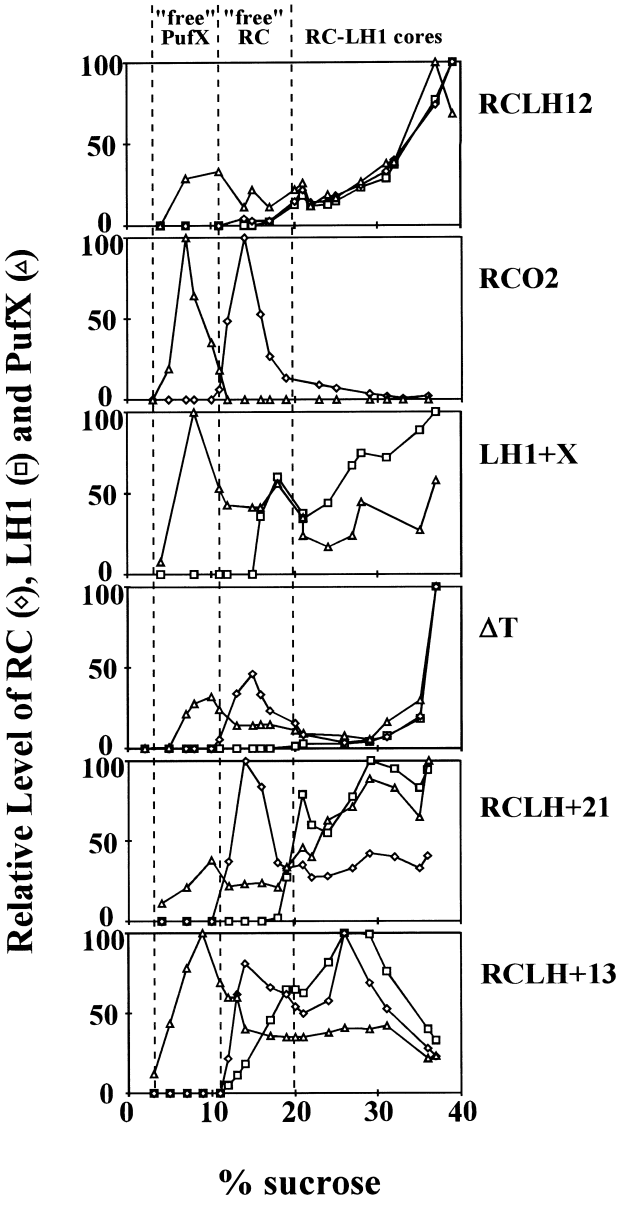

Fig. 3. Analysis of detergent-solubilised proteins from the core mutants. The pigment–protein complexes were separated by centrifugation on sucrose gradients to show the relative level of RC (diamonds), LH1 (squares) and PufX protein (triangles).

membranes from strain ΔT contain cores with an apparent, mean core size of ~14, it is likely that this masks the existence of a substantial proportion of antenna-free RCs in the membrane, with the remainder in RC–LH1 complexes with an average composition of 21 LH1 Bchls per RC.

Fig. 3 also shows that this method can efficiently separate the PufX polypeptide from the RC; in the LH1-deficient strain, RCO2, the main fraction of RCs was found between 10 and 20% sucrose, whereas the distribution of PufX was quite distinct from this (denoted as 'free' PufX). This demonstrates that, under these conditions, PufX shows little affinity for the RC. A considerable amount of free PufX was also seen in the RC-deficient strain LH1+X. The remaining PufX protein was distributed, along with the LH1 complex, in the 15–40% region of the gradient; the simplest interpretation of this is that the PufX protein found in these fractions is associated with the LH1 complex. In gradients prepared from membranes of the control strain RCLH12, the majority of the PufX found was associated with both LH1 and RCs in the region between 20 and 40% sucrose. We assume that most of the RC and LH1 found in this region is associated together in the core complexes, with PufX.

Taken together, the solubilisation results for the three strains RCO2, RCLH12, and LH1+X suggest that the PufX polypeptide is tightly bound to the normal LH1–RC core in membranes of the RCLH12 strain, and that when one of these components of the RC:LH1 core is absent, the mild solubilisation method used is effective in producing significantly increased amounts of 'free' PufX. Therefore, this experiment reveals a hierarchy of binding capacity for the PufX polypeptide in the order RC:LH1 > LH1 > RC.

Comparison of the solubilisation data for the C-terminal truncation strains RCLH+21 and RCLH+13 in Fig. 3 clearly shows that PufX is more loosely attached to the RC:LH1 core complexes of strain RCLH+13. Possible implications of this are considered in the Discussion.

3.3. *Time-dependent assembly of the photosynthetic apparatus of Rb. sphaeroides*

In order to gain some more information on the relationship of PufX to other components of the RC:LH1 core complex, the time course of assembly of the photosynthetic apparatus was analysed in the wild-type strain NCIB 8253. It has been known for many years that the time-dependent assembly of photosynthetic membranes in *Rb. sphaeroides* can be studied by inducing the synthesis of the lipid, protein and pigment components of the photosyn-

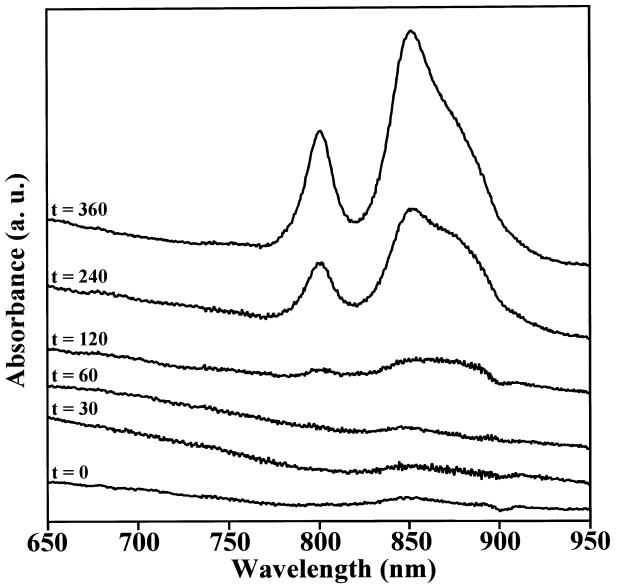

Fig. 4. Room temperature absorbance spectra of whole cells of *Rb. sphaeroides* NCIB 8253 after induction of semi-aerobic photosynthetic growth, where $t=0$ is the start of induction, and $t=30$, 60, 120, 240 and 360 are the time in minutes after induction of photosynthetic growth.

thetic apparatus in the dark, under limiting oxygen [37]. Under these conditions, the synthesis of invaginations of the cytoplasmic membrane which house the photosynthetic complexes occurs over a time scale of around 12 h. The present experiment was confined to the first 400 min of the process, which is known to be the time when the components of the LH1–RC core complex are preferentially synthesised [37,52]. In this way, it was hoped that it would be possible to observe the sequence of assembly of PufX in relation to the rest of the core.

A culture of the wild-type *Rb. sphaeroides* strain was grown in the dark under conditions where oxygen was not limiting and then transferred to fresh medium and grown under oxygen-limited conditions in the dark (see Section 2). Samples were removed from the culture at intervals over the first 400 min of oxygen-limited growth and used to prepare RNA and protein cell extracts, and samples for absorbance spectroscopy. Under these conditions, as the spectra in Fig. 4 indicate, the photosynthetic apparatus assembles, with LH1 (absorbing at 875 nm) tending to predominate in the early stages. Later on, LH2, absorbing at 800 and 850 nm, is more in evidence. Northern and Western blots were probed for transcripts and proteins, respectively, for the LH2 antenna, LH1 antenna, the RC and the PufX protein, and the resulting Northern and immunodetection autoradiograms were scanned and the optical density values calculated. The percentage of RNA and protein at each time point was calculated by assigning the highest value observed for each as 100%.

Examination of the variations in the levels of the protein components of the photosynthetic unit over time shows that PufX protein is present 50 min after induction, 100 min before the LH1α protein is apparent (Fig. 5A). Thus the rise in PufX protein is more immediate, whereas LH1α, the product of the *pufBA* transcript, appears to be subject to a relative lag. In contrast, both subunit H of the RC and subunit IV of the cyt bc_1 complex are present before the onset of

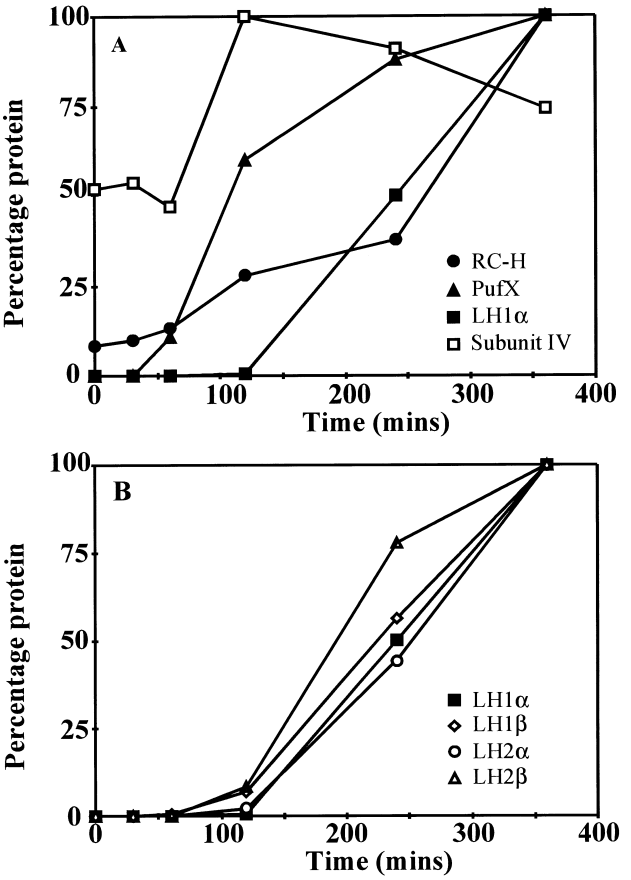

Fig. 5. Presence of protein components of the photosynthetic unit in *Rb. sphaeroides* NCIB 8253 over time after induction of semi-aerobic photosynthetic growth. The amount of each protein is calculated by assigning the highest value observed as 100% and expressing all other values relative to this.

photosynthetic growth, increasing over time, but with differing rates. Both subunit IV and the PufX protein can be seen to undergo a parallel, rapid rise in the total percentage protein between 60 and 120 min, whereas the RC-H subunit exhibits a steady increase in protein up to 240 min, and then more than doubles from 38 to 100% in the final 120 min time interval. Interestingly, it can be seen that the total percentage of LH1α and LH1β protein also doubles over the final 120 min (Fig. 5B) suggesting that an increase in the level of LH1 proteins accompanies, and is possibly related to, an increase in the translation of subunit H mRNA (*puhA*). For example, the formation of functional RC–LH1 core complexes could result in a depletion of free subunit H protein, which itself may act as a trigger to increase translation.

Fig. 5B also shows that LH1β and LH2β are present before the α subunit of each of these polypeptides. However, it should be noted that the levels of polypeptide detected in mutants do not necessarily correspond to functional LH complexes, because Western analysis of these developing membranes also detects proteins that are not bound to Bchl.

As both the protein and RNA examined in this experiment were prepared from the same sample it was possible to make a direct comparison of the onset of accumulation of the transcripts with the presence of the protein encoded by these transcripts (Fig. 6). In the case of *pufX* (Fig. 6A) it can be seen that the onset of appreciable increases in the *pufBALMX* transcript, between 30 and 120 min, occurs prior to such an increase in the level of PufX protein, which is seen between 60 and 240 min, as would be expected for protein production. A similar effect is also seen for the *pufBA*-probed 0.5 kb transcript and its products, LH1α and LH1β (Fig. 6B). The differences between the amounts of large (*pufBALMX*) and small (*pufBA*) transcripts are reflected in the rises that are also seen in the levels of LH1 polypeptides (Fig. 6B). As discussed below, the timing of the delay in the amount of *pufBA* protein products with respect to the large transcript may reflect the need of the system to establish a RC–PufX–LH$\alpha_1\beta_1$ complex from the large transcript prior to its encirclement by the product of the *pufBA* small transcript, LH1α and LH1β.

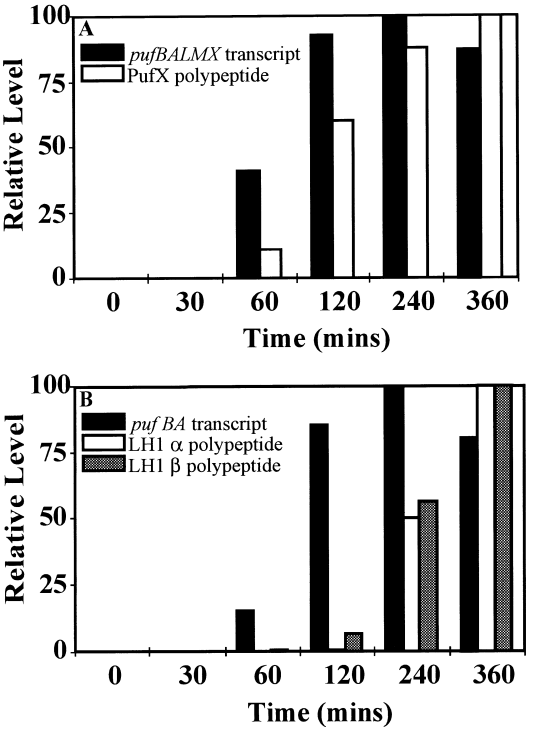

Fig. 6. Histograms to show the variation in level of RNA transcript and protein in *Rb. sphaeroides* NCIB 8253 after induction of semi-aerobic photosynthetic growth.

3.4. Determination of the topology of the PufX polypeptide in intracytoplasmic membranes of the wild-type strain

Having shown that the insertion of the PufX protein precedes that of the LH1 complex, it was of interest to determine the topology of PufX within the membrane. Proteolytic treatment of chromatophores, which are uniformly orientated intracytoplasmic vesicles arising from the disruption of cells of *Rb. sphaeroides* wild-type strains [53,54] should facilitate determination of the topology of PufX, by digestion of proteolytically accessible domains of the protein, followed by protein sequencing.

Chromatophore membranes of *Rb. sphaeroides* strain NCIB 8253 were prepared on continuous sucrose gradients as described by Niederman et al. [55] and these were incubated with prot K, in a prot K to protein ratio of 1:30, for increasing lengths of time. Prot K has a broad substrate specificity, and can be completely inhibited with PMSF; in previous studies [56] prot K has been shown to digest many proteins, but not to destroy the structural integrity of chroma-

tophores, nor to penetrate intact membranes. Membrane samples from the digestion were then analysed by sodium dodecyl polyacrylamide gel electrophoresis in duplicate. One gel was stained with Coomassie brilliant blue and the other was used either for Western blotting and immunodetection with antisera specific for subunit H of the RC, LH1α polypeptide and PufX polypeptide, or sequence analysis by N-terminal Edman degradation.

Initial examination of all the time points, (0, 5, 10, 20, 40, 60, 80 and 100 min) by immunodetection of samples with PufX – specific antibodies highlighted the presence of a possible cleavage product of PufX after 20 min incubation with prot K at 30°C (not shown). A duplicate Coomassie blue stained gel was used to clarify that all the lane loadings were equal. However, our inability to stain the PufX peptide in SDS-PAGE emphasises the absolute requirement of immunodetection for identifying and isolating PufX. From the above data the PufX polypeptide remaining after 80 min of prot K digestion was chosen for N-terminal sequencing. Prot K-digested membranes, undigested chromatophores, and membranes from control strains RCLH12 and RCLH12X$^-$ were each separated by SDS-PAGE in duplicate, and one of the gels was blotted onto PVDF sequencing membrane and stained with Coomassie blue R-250. In order to locate PufX and enable the correct bands to be excised from the sequencing membrane for analysis the second duplicate gel was blotted onto nitrocellulose for Western analysis and the immunoreactive bands were highlighted by alkaline phosphatase colour immunodetection (see Fig. 7ii). The sample of undigested PufX protein was found to lack the N-terminal methionine residue but otherwise the sequence was as expected for wild-type PufX, whereas the sequence from the upper PufX band of the 80 min digest sample was truncated by seven amino acid residues after the N-terminal methionine (see Fig. 7i). The lower PufX immunoreactive band in the 80 min digest sample was also sequenced, but no homology to any region of PufX was found.

Prot K treatment resulted in no alteration of the gel position of the LH1α immunoreactive band, with band intensity decreasing only after long periods of treatment. In addition, the LH2α band from untreated chromatophores and chromatophores treated with prot K for 80 min showed no difference in N-terminal amino acid sequence, confirming results of Tadros et al. [56]. The LH1β polypeptide was shown to be truncated by four N-terminal amino acids (Asp, Ser, Ala, Lys) after treatment with prot K for 80 min, confirming the results of Takemoto et al. [57], who showed cleavage of LH1β between positions 4 and 5 from the N-terminal end on the chromatophore surface, but no cleavage of the LH1α polypeptide.

In addition to LH1β, the RC subunit H polypeptide was used as a second marker of the cytoplasmic membrane surface, as the topology of the RC is known [58]. Immunodetection with RC subunit H specific antibodies showed that prot K cleaves a small fragment of approximately 1–2 kDa from the H subunit protein (data not shown) as described previously by Theiler and Neiderman [58].

It can be concluded from these results that the product of the *pufX* gene is N-terminally exposed on the cytoplasmic surface of the photosynthetic membrane. This is consistent with the prediction based on von Heijne's 'positive inside' rule [39], that the N-terminus of PufX would be expected to be cytoplasmic and the C-terminus periplasmic if in fact PufX is a membrane-spanning protein as is suggested by hydropathy analysis [29]. The alternative explanation is that PufX is entirely associated with the cytoplasmic surface of the intracytoplasmic membrane and does not traverse it. In such a case, the majority of PufX, would have to be inaccessible to the protease.

4. Discussion

4.1. The presence of LH1 is essential for the correct binding of PufX to the core

The effects of solubilisation on the localisation of PufX in sucrose gradients for the control strains RCO2, RCLH12 and LH1+X (Fig. 3) enable us to propose a hierarchy of binding capacity for PufX to the core of RC:LH1 > LH1 > RC, where antenna-free RCs in the RC-only strain RCO2 have virtually no capacity to bind PufX. Hence this hierarchy suggests that the ability to bind PufX is a property of the LH1 polypeptides, and is conferred to the RCLH12 strain by the presence of LH1. A compar-

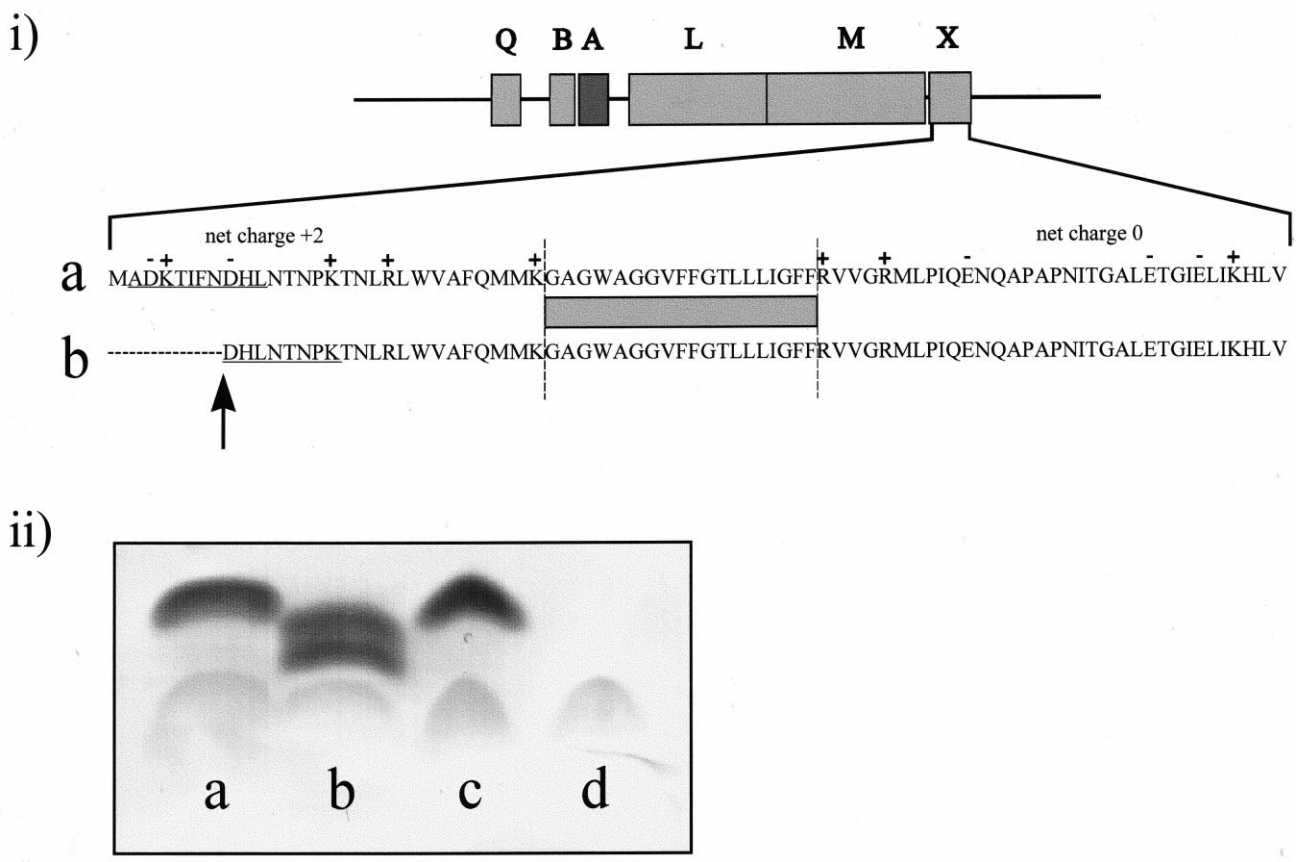

Fig. 7. Digestion of PufX with proteinase K for topology studies. (i) Sequence analysis of the N-terminus of PufX. The sequence of the 80 min prot K digest sample, truncated by seven amino acid residues, is shown below the wild-type sequence of PufX. In each case, the underlined region denotes the residues that were actually sequenced. (ii) Immunodetection of PufX polypeptide in control and digested samples. Lanes: a, undigested wild-type chromatophores; b, wild-type chromatophores after 80 min digestion with prot K; c, RCLH12 control chromatophores; d, RCLH12X$^-$ control chromatophores.

ison of RCLH+21 and RCLH+13 suggests that the mild solubilisation is more effective in producing a 'free' PufX fraction from membranes of RCLH+13. The simplest explanation of this difference lies in the deletion of eight extra residues from the C-terminal region of the LH1α polypeptide in strain RCLH+13. It is possible that there might be an area of association between the LH1α and PufX polypeptides in this C-terminal region.

4.2. *When LH1 is present in limiting and subnormal amounts, it is not distributed evenly among the cores*

The 'small core' mutants created either by removal of the intercistronic *pufA–L* stem-loop structure (mutants ΔT, ΔTΔX) or by truncating the LH1α polypeptide (RCLH+21 and RCLH+13) were analysed by limited fractionation of the cores in sucrose/detergent gradients (Table 1 and Fig. 3). The data presented above indicated that RC–LH1 core complexes containing wild-type LH1α and β polypeptides can assemble with reduced ratios of LH1:RC, and indicate that previous data in which similar RC–LH1 core complexes were obtained with mutant LH1α polypeptides [33] were not artefacts of the C-terminal deletions in the LH1α polypeptide. Thus core complexes with reduced LH1:RC ratios can be obtained merely by a reduction in the expression of the *pufBA* genes. Several models of RC–LH1 complexes have been proposed in which the RC is surrounded by a ring of LH1 [8,10,13,14]; the finding that RC–LH1 complexes can exist and perform energy transfer with reduced LH1:RC ratios has implications for such a

structure. Assuming that there are essential specific contacts between the RC and the inner face of an LH1 ring, the presumed maintenance of such contacts upon reduction of the number of LH1 heterodimers within the ring suggests that the ring has sufficient structural flexibility to enable it to accommodate such changes.

4.3. The assembly of the core complex: PufX associates with the RC in the membrane bilayer, prior to encirclement of the RC by LH1

The time course experiment (Figs. 4–6) reveals some more details of the assembly of components of the photosynthetic unit and enables us to propose a sequence of assembly for PufX in relation to the rest of the core. Under the conditions chosen for this experiment, in which highly aerated cells containing almost no photosynthetic complexes are induced to start the assembly process by a switch to low aeration in the dark, the formation of the core seems likely to start at the positions in the cell where the RC-H subunit is found, since at time zero, this is the only detectable part of the photosynthetic unit. This result is consistent with earlier work by Chory et al. [38], who showed that highly aerated cells contain RC-H and proposed that RC-H was, therefore, a likely starting point for this process. Transcription of the *pufB*, *A*, *L*, *M* and *X* is seen to be closely followed by translation of these genes and the appearance of the *pufX*, then *pufBA* gene products (Figs. 5 and 6). It is clear that higher relative amounts of the PufX polypeptide are synthesised before LH1α and β make an appearance. Fig. 5B also demonstrates that there are significant differences between the onset of synthesis of the β and α polypeptides, particularly in the case of LH2, where the synthesis of the α polypeptide lags behind β. As far as the assembly of the LH1–RC core complex is concerned, the delay in achieving the maximal levels of LH1α and LH1β with respect to PufX may reflect the need of the system to establish a compact RC–PufX–LH1$\alpha_1\beta_1$ complex from the large transcript prior to its encirclement by the product of the *pufBA* small transcript, LH1α and LH1β. These results suggest that the PufX protein is an important component in the assembly process, and by considering this protein as a docking protein for LH1, we can propose that PufX associates with the RC and a limited amount of LH1α and β in the membrane bilayer, prior to encirclement of the RC by the rest of the LH1 complex, despite the apparent absence of interaction between the detergent solubilised RC and PufX protein in vitro (Fig. 3, RCO2). In this model, we propose that initially the LH1 subunits associate with the RC as an incomplete ring, with PufX acting as an initial recognition site on the RC and a possible starting point for the encirclement process.

4.4. The N-terminus of PufX is exposed at the cytoplasmic surface of the membrane

PufX inserts in the membrane so that the N-terminus is exposed on the cytoplasmic surface of the membrane, and if we assume that it contains a single transmembrane span then it is a monotopic N_{in}–C_{out} membrane protein, according to the terminology of von Heijne [39]. This proposed topology of PufX is consistent with the prediction from von Heijne's 'positive inside' rule [39] since an inspection of the sequence (Fig. 7i) shows a net positive charge on the N-terminal side of the putative membrane-spanning region. The removal of the sequence ISAAKYNR from +21 to +13 at the C-terminus of LH1α produces a large increase in the amount of PufX liberated from solubilised cores prepared from the C-terminal truncation strains RCLH+21 and RCLH+13 (Fig. 3). However, since we can assume that both the LH1α and β polypeptides are monotopic N_{in}–C_{out} membrane proteins, it is reasonable to propose that the effect of deleting residues at the C-terminus of LH1α arises because PufX shares this same topological arrangement with LH1α and β. Therefore, we favour the transmembrane model, as opposed to one in which PufX resides entirely on the cytoplasmic face of the membrane, with only the N-terminus susceptible to digestion with prot K. The data in Fig. 3 then led to the possibility that the C-terminal end of LH1α may be a vital recognition and/or binding site for the C-terminal end of the PufX peptide.

4.5. A possible role for the B820 subunit of LH1 in the assembly of the core

Several results obtained in this work led to the conclusion that there can be incomplete rings of

LH1, and that LH1 is a major factor in the stabilisation of PufX in the membrane despite the fact that there is very little LH1 available at the earliest stages of the assembly of the core complex. One explanation of these results is that there is a modular assembly and structure for LH1, in which the basic unit for assembly is an LH1$\alpha_1\beta_1$Bchl$_2$ complex. It is possible that a RC–PufX–(LH1$\alpha_1\beta_1$Bchl$_2$) complex is formed initially at the earliest stages of the assembly of the core, and also that LH1$\alpha_1\beta_1$Bchl$_2$ units are progressively added to this complex, resulting, ultimately, in the encirclement of the RC. In support of this, it has been established that LH1 complexes from a variety of bacteria can be reversibly dissociated into a B820 complex in the presence of detergents, often β-octyl glucoside, and that the minimum size of such a unit is $\alpha_1\beta_1$Bchl$_2$ [59]. This is a stable complex, and is the building block of LH1 in vitro, and so it is possible that it might fulfil a similar role in vivo. Another piece of evidence that LH1 might be progressively assembled from B820 units is that in the presence of the detergent lithium dodecyl sulphate (LDS) the LH1 complex can be fractionated by polyacrylamide gel electrophoresis, forming a ladder of Bchl-containing complexes, each band in the gel differing from the next by the mass of one $\alpha_1\beta_1$Bchl$_2$ unit [46,60,61]. The forces stabilising the formation of a $\alpha_1\beta_1$Bchl$_2$ unit are conferred by the network of H-bonds revealed by resonance Raman studies of site-directed mutants of LH1 [41,62,63], in which the four possible H-bonds to the pair of Bchls are donated by the α and β polypeptides that bind the same Bchls. Thus, these four H-bonds are 'internal' to the B820 unit, and provide a significant driving force to stabilise this complex [64]. It should be noted that the analogous H-bonding arrangement in LH2 from *R. sphaeroides* and *R. acidophila* is not of this type [6,65], and possibly as a consequence of this it has not been possible to dissociate these complexes into $\alpha_1\beta_1$Bchl$_2$ units. A further consequence of this might be a different mode of assembly of the LH2 complex.

Acknowledgements

This work was supported by the Human Frontier Science Program. R.J.P. gratefully acknowledges a studentship from the Biotechnology and Biological Sciences Research Council. M.R.J. is a BBSRC Advanced Research Fellow. The authors are grateful to Professors Richard Cogdell and Robert Niederman for gifts of antibodies, and to Grant Naylor for technical support.

References

[1] J. Aagaard, W.R. Sistrom, Photochem. Photobiol. 15 (1972) 209–225.
[2] J. Deisenhofer, O. Epp, K. Miki, R. Huber, H. Michel, Nature 318 (1985) 618–624.
[3] C.-H. Chang, D. Tiede, J. Tang, U. Smith, J. Norris, M. Schiffer, FEBS Lett. 205 (1986) 82–86.
[4] C.-H. Chang, O. El-Kabbani, D. Tiede, J. Norris, M. Schiffer, Biochemistry 30 (1991) 5352–5360.
[5] G. Feher, J.P. Allen, M.Y. Okamura, D.C. Rees, Nature 339 (1989) 111–116.
[6] G. McDermott, S.M. Prince, A.A. Freer, A.M. Hawthornthwaite-Lawless, M.Z. Papiz, R.J. Cogdell, N.W. Isaacs, Nature 374 (1995) 517–521.
[7] J. Koepke, X. Hu, C. Muenke, K. Schulten, H. Michel, Structure 4 (1996) 581–597.
[8] S. Karrasch, P.A. Bullough, R. Ghosh, EMBO J. 14 (1995) 631–638.
[9] H. Savage, M. Cyrklaff, G. Montoya, W. Kühlbrandt, I. Sinning, Structure 4 (1996) 243–252.
[10] I. Ikeda-Yamasaki, T. Odahara, K. Mitsuoka, Y. Fujiyoshi, K. Murata, FEBS Lett. 425 (1998) 505–508.
[11] R.U. Meckenstock, K. Krusche, L.A. Staehelin, M. Cyrklaff, H. Zuber, Biol. Chem. 375 (1994) 429–438.
[12] A.F. Boonstra, R.W. Visschers, F. Calkoen, R. van Grondelle, E.F.J. van Bruggen, E.J. Boekema, Biochim. Biophys. Acta 1142 (1993) 181–188.
[13] A.F. Boonstra, L. Germeroth, E.J. Boekema, Biochim. Biophys. Acta 1184 (1994) 227–234.
[14] T. Walz, R. Ghosh, J. Mol. Biol. 265 (1997) 107–111.
[15] J.C. Williams, L.A. Steiner, R.C. Ogden, M.I. Simon, G. Feher, Proc. Natl. Acad. Sci. USA 80 (1983) 6505–6509.
[16] J.C. Williams, L.A. Steiner, G. Feher, M.I. Simon, Proc. Natl. Acad. Sci. USA 81 (1984) 7303–7308.
[17] P.J. Kiley, T.J. Donohue, W.A. Havelka, S. Kaplan, J. Bacteriol. 169 (1987) 742–750.
[18] C.N. Hunter, P. McGlynn, M.K. Ashby, J.G. Burgess, J.D. Olsen, Mol. Microbiol. 5 (1991) 2649–2661.
[19] C.E. Bauer, B.L. Marrs, Proc. Natl. Acad. Sci. USA 85 (1988) 7074–7078.
[20] J.W. Farchaus, W.P. Barz, H. Grünberg, D. Oesterhelt, EMBO J. 11 (1992) 2779–2788.
[21] T.G. Lilburn, C.E. Haith, R.C. Prince, J.T. Beatty, Biochim. Biophys. Acta 110 (1992) 160–170.
[22] P. McGlynn, C.N. Hunter, M.R. Jones, FEBS Lett. 349 (1994) 349–353.
[23] W.P. Barz, F. Francia, G. Venturoli, B.A. Melandri, A.

Vermeglio, D. Oesterhelt, Biochemistry 34 (1995) 15235–15247.
[24] W.P. Barz, F. Francia, G. Venturoli, B.A. Melandri, A. Vermeglio, D. Oesterhelt, Biochemistry 34 (1995) 15248–15258.
[25] Y.S. Zhu, S. Kaplan, J. Bacteriol. 162 (1985) 925–932.
[26] Y.S. Zhu, P.J. Kiley, T.J. Donohue, S. Kaplan, J. Biol. Chem. 261 (1986) 10366–10374.
[27] B.S. DeHoff, J.K. Lee, T.J. Donohue, R.I. Gumport, S. Kaplan, J. Bacteriol. 170 (1988) 4681–4692.
[28] L. Gong, S. Kaplan, Microbiology 142 (1996) 2057–2069.
[29] J.K. Lee, B.S. Dehoff, T.J. Donohue, R.I. Gumport, S. Kaplan, J. Biol. Chem. 264 (1989) 19354–19365.
[30] G. Klug, C.W. Adams, J. Belasco, B. Doerge, S.N. Cohen, J. Bacteriol. 172 (1987) 5140–5146.
[31] G. Klug, Mol. Microbiol. 9 (1993) 1–7.
[32] D.G. Youvan, E.J. Bylina, M. Albert, H. Begusch, J.E. Hearst, Cell 37 (1984) 949–957.
[33] P. McGlynn, W.H.J. Westerhuis, M.R. Jones, C.N. Hunter, J. Biol. Chem. 271 (1996) 3285–3292.
[34] T.G. Lilburn, J.T. Beatty, FEMS Microbiol. Lett. 100 (1992) 155–160.
[35] W.P. Barz, D. Oesterhelt, Biochemistry 33 (1994) 9741–9752.
[36] T.G. Lilburn, R.C. Prince, J.T. Beatty, J. Bacteriol. 177 (1995) 4593–4600.
[37] R.A. Niederman, D.E. Mallon, J.J. Langan, Biochim. Biophys. Acta 440 (1976) 429–447.
[38] J. Chory, T.J. Donohue, A.R. Varga, L.A. Staehelin, S. Kaplan, J. Bacteriol. 159 (1984) 540–554.
[39] G. von Heijne, J. Mol. Biol. 225 (1992) 487–494.
[40] C.N. Hunter, G. Turner, J. Gen. Microbiol. 134 (1988) 1471–1480.
[41] J.D. Olsen, G.D. Sockalingum, B. Robert, C.N. Hunter, Proc. Natl. Acad. Sci. USA 91 (1994) 7124–7128.
[42] M.R. Jones, R.W. Visschers, R. van Grondelle, C.N. Hunter, Biochemistry 31 (1992) 4458–4465.
[43] M.R. Jones, J.G.S. Fowler, L.C.D. Gibson, G.G. Grief, J.D. Olsen, W. Crielaard, C.N. Hunter, Mol. Microbiol. 6 (1992) 1173–1184.
[44] J. Sambrook, E.F. Fritsch, T. Maniatis, Molecular Cloning. A Laboratory Manual, 2nd edn., Cold Spring Harbor Laboratory Press, Cold Spring Harbor, NY, 1989.
[45] M.R. Jones, M. Heer-Dawson, T.A. Mattioli, C.N. Hunter, B. Robert, FEBS Lett. 339 (1994) 18–24.
[46] C.N. Hunter, J.D. Pennoyer, J.N. Sturgis, D. Farrelley, R.A. Niederman, Biochemistry 27 (1988) 3459–3467.
[47] D. Molenaar, W. Crielaard, K.J. Hellingwerf, Biochemistry 27 (1988) 2014–2023.
[48] M. van der Rest, G. Gingras, J. Biol. Chem. 249 (1974) 6446–6453.
[49] H. Schägger, G. von Jagow, Anal. Biochem. 166 (1987) 368–379.
[50] K.P. Smith, R.I. Krohn, G.T. Hermanson, A.K. Mallia, F.H. Gartner, M.D. Provenzano, E.K. Fujimoto, N.M. Goeke, B.J. Olsen, D.C. Klenck, Anal. Biochem. 150 (1985) 76–85.
[51] N. LeGendre, P. Matsudaira, in: P. Matsudaira (Ed.), A Practical Guide To Protein and Peptide Purification For Microsequencing, Academic Press, London, 1989, pp. 49–69.
[52] C.N. Hunter, M.K. Ashby, S.A. Coomber, Biochem. J. 247 (1987) 489–492.
[53] R.A. Niederman, K.D. Gibson, in: R.K. Clayton, W.R. Sistrom (Eds.), The Photosynthetic Bacteria, Plenum Press, New York, 1978, pp. 79–118.
[54] J. Takemoto, R.C. Bachmann, Arch. Biochem. Biophys. 195 (1979) 526–534.
[55] R.A. Niederman, D.E. Mallon, L.C. Parks, Biochim. Biophys. Acta 555 (1979) 210–220.
[56] M.H. Tadros, R. Frank, J.Y. Takemoto, G. Drews, J. Bacteriol. 170 (1988) 2758–2762.
[57] J.Y. Takemoto, R.L. Peterson, M.H. Tadros, G. Drews, J. Bacteriol. 169 (1987) 4731–4736.
[58] R. Theiler, R.A. Neiderman, J. Biol. Chem. 266 (1991) 23163–23168.
[59] P.A. Loach, P.S. Parkes-Loach, in: R.E. Blankenship, M.T. Madigan, C.E. Bauer (Eds.), Anoxygenic Photosynthetic Bacteria, Vol. 2, Kluwer Academic, Dordrecht, 1995, pp. 437–471.
[60] R.M. Broglie, C.N. Hunter, P. Delepelaire, R.A. Niederman, N.H. Chau, R.K. Clayton, Proc. Natl. Acad. Sci. USA 77 (1980) 87–91.
[61] W.H.J. Westerhuis, Pigment Organisation and Oligomeric Protein Structure of the Light-Harvesting Complexes of Purple Bacteria, Ph.D. thesis, Rutgers University, New Jersey, USA, 1994.
[62] J. Sturgis, J.D. Olsen, B. Robert, C.N. Hunter, Biochemistry 36 (1997) 2772–2778.
[63] J.D. Olsen, J. Sturgis, C.N. Hunter, B. Robert, Biochemistry, in press.
[64] C.M. Davis, P.L. Bustamante, J.B. Todd, P.S. Parkes-Loach, P. McGlynn, J.D. Olsen, L. McMaster, C.N. Hunter, P.A. Loach, Biochemistry, in press.
[65] G.J.S. Fowler, G.D. Sockalingum, B. Robert, C.N. Hunter, Biochem. J. 299 (1994) 695–700.